Response to Reviewers' comments

Reviewer 2

This manuscript presents an analysis of atmospheric VOCs in Guangzhou over roughly a two-month intensive sampling period, Sept-Nov 2016. The authors use the significant uncalibrated and/or unattributed ion response from a high-resolution PTR-MS instrument to estimate the total OH reactivity and compare this quantity to a direct measurement.

This type of analysis has been published previously, as the authors acknowledge and rely upon as a basis for their own work. The combination of the setting of their mea- surements in the Pearl River Delta and the use of a state-of-the-art instrument make this manuscript scientifically important. The writing is clear and presented in a logical format.

Generally, this manuscript is missing error analysis and an adequate description of the many ions that were observed. The authors often will make a simplifying assumption for their data to ease their analysis, but either do not provide enough information to allow the reader to evaluate this assumption (e.g. OH reactivities of detected ions) or perhaps over-simplify in spite of their own data indicating a more detailed analysis is warranted (e.g. assumed sensitivities). The authors provide only cursory description of measurement uncertainties, and instead rely upon the observed dynamic range of reported mixing ratios or signal in section 3.3 (Sources analysis of OVOCs). Even these ranges are dropped in 3.4 (OH Reactivity) and the results from this section, which hinge upon numerous assumptions presented earlier, are stated with far greater precision than is merited. This can be contrasted with other manuscripts that have previously presented this type of analysis (e.g. De Gouw et al., 2009) that the authors cite.

While I do have some criticisms of this manuscript, I believe that this work should be accepted for publication with revisions to address these issues.

Reply: We are very grateful for all the detailed comments and the valuable suggestions, which helped us greatly in improving our manuscript. Please find the response to individual comments below.

Regarding of error analysis suggested by the reviewer, we have provided more

related information in the revised manuscript. In this manuscript, our main conclusion is the important roles of oxygenated species in VOCs in terms of both concentrations and OH reactivity. This conclusion heavily rely on quantificaiton of the uncalibrated species in the mass spectra of PTR-ToF-MS. As a result, the main uncertainty throughout the analysis in section 3.3 and section 3.4 comes from the errors in both concentration and OH rate constants of these uncalibrated species.

For the determination of sensitivity for uncalibrated species by PTR-ToF-MS, we re-checked the relationship between sensitivity and rate constants for proton-transfer reactions of H_3O^+ with VOCs. We obtained reasonable correlation, after considering the effect of higher energetic collisions on rate constant for proton-transfer reactions in the drift tube. This relationship is used to calculate sensitivities for uncalibrated species by PTR-ToF-MS. The quantification for these uncalibrated species would be more reasonable than using the average response from calibrated VOCs. Following the discussions in previous studies, the uncertainties for concentrations of these uncalibrated species are around 50%. We explicitly include this information in the revised manuscript and discuss the effects in the analysis of section 3.3 and 3.4.

For the rate constants of VOCs in calculating OH reactivity, the values of various VOCs are taken from previous literatures (Atkinson and Arey, 2003;Atkinson et al., 2004;Atkinson et al., 2006;Koss et al., 2018). For ions detected by PTR-ToF-MS, the rate constants of the determined or assumed dominant isomers are used, following identification of these ions in previous studies (Koss et al., 2018;Gilman et al., 2015). As the attribution of various ions to specific compounds are not explicitly available for many ions detected by PTR-ToF-MS, the uncertainties of rate constants of many ions can be large, especially for the uncalibrated species. Considering large differences between OH rate constants for isomers (e.g. ketone vs aldehyde), we believe the uncertainty in rate constants can be on the order of 100%. The effect of this uncertainty in missing reactivity is included in the revised manuscript.

As discussed in section 2.2, a total of 31 VOCs species were calibrated using either gas cylinders or liquid standards. For other VOCs, we used the method proposed in Sekimoto et al. (2017) to determine the relationship between VOCs sensitivity and kinetic rate constants for proton-transfer reactions of H_3O^+ with VOCs (detailed discussions in the SI). As shown in Figure 3, a clear linear relationship was obtained. The fitted line in Figure 3 is used to determine sensitivities of the uncalibrated species. Following the discussions in Sekimoto et

al. (2017), uncertainties of the concentrations for uncalibrated species are around 50%.

Adding up these contributions, it significantly narrows the gap between the measured and calculated OH reactivity, leaving only 11% of OH reactivity as "missing" during the campaign. Considering the large uncertainties for both concentrations (~50%) and rate constants of the uncalibrated species (on the order of 100%), the missing reactivity can ranged in 0%-19%. Nevertheless, the determined missing reactivity would be well below the estimated uncertainty (20%) for the OH reactivity measurements by the CRM method, indicating that gap between measured and calculated reactivity can be significantly narrowed after taking into account all of the species by PTR-ToF-MS.

Specific comments

Line 39-44. The authors cite a number of percentage contributions of OVOCs, HCs, etc. to the total VOC burden. These values are overly precise and lack a statement of uncertainty. Uncertainties should be in the abstract, and significant digits should be made appropriate based upon those uncertainties.

Reply: Thanks for the reminder.

These values have been modified to:

OVOC-related ions dominated PTR-ToF-MS mass spectra with an average contribution of 73%±9%. Combining measurements from PTR-ToF-MS and GC-MS/FID, OVOCs contribute 57%±10% to the total concentration of VOCs. Using concurrent measurement of OH reactivity, OVOCs measured by PTR-ToF-MS contribute greatly to the OH reactivity (19%±10%). In comparison, hydrocarbons account for 21%±11% of OH reactivity. Adding up the contributions from inorganic gases (48%±15%), ~11% of the OH reactivity remains as "missing".

Line 108. "Field measurements were conducted . . ." Figure S1 shows a map of the local region but is never cited in the text.

Reply: We have cited Figure S1 in the revised manuscript.

Field measurements were conducted at an observation site in Guangzhou (113.2°E, 23°N) from September to November 2018. The sampling site (~25 m above the ground level) is located on the 9th floor of a building on the campus of Guangzhou Institute of Geochemistry, Chinese Academy of Sciences, which is

regarded as a typical urban site in Guangzhou (Figure S1).

Line 114. "commercial PTR-QiTof-MS". The authors should provide a brief description of this instrument, specifically with regards to the meaning of "QiToF".

Reply: This description has been added in the Section 2 of the revised manuscript.

During the campaign, a commercial PTR-QiToF-MS (Ionicon Analytic GmbH, Innsbruck, Austria) with H_3O^+ chemistry and NO^+ chemistry was used to measure VOCs in the atmosphere. PTR-QiToF-MS is equipped with a quadrupole ion guide for effective transfer of ions from the drift tube to the time-of-flight mass spectrometer, and "Qi" here stands for "quadrupole interface" (Sulzer et al., 2014). It has been shown that the new quadrupole interface greatly improves sensitivity of VOC detection (Sulzer et al., 2014).

Line 116. "Ambient air was continuously . . ." Figure S2 shows the plumbing scheme for the instrument but is never cited in the text.

Reply: We have cited it in the revised manuscript.

Ambient air was continuously introduced through an 8 m long PFA Teflon tubing (1/4") into PTR-ToF-MS with an external pump (5.0 L/min) (Figure S2).

Line 117. "Teflon tubing" Which type of Teflon tubing is this (e.g. PFA, FEP, PTFE)?

Reply: The type of Teflon tubing is PFA. We have indicated it in the revised manuscript.

Ambient air was continuously introduced through an 8 m long PFA Teflon tubing (1/4") into PTR-ToF-MS with an external pump (5.0 L/min) (Figure S2). The PFA Teflon tubing was wrapped with a self-controlled heater wire (40 °C) to prevent air condensation inside the tubing.

Line 119-120. "the PTR-ToF-MS automatically switched between H3O+ and NO+ chemistry every 10-20 minutes" The authors should provide a description of how this was accomplished, or a reference if this was previously published.

Reply: We included more details about the automatic switches between H_3O^+ chemistry and NO^+ chemistry in the revised manuscript:

During the campaign, the PTR-ToF-MS automatically switched between

H_3O^+ and NO^+ chemistry every 10-20 minutes. The built-in PTR-manager software (Ionicon Analytic GmbH, Innsbruck, Austria) offers the possibility to set programed sequences for switching between the two reagent ions. It takes ~10 s for $H_3O^+$and ~20 s for NO^+ to re-equilibrate, when the measurement automatically switches between these two modes. The ambient measurement data during the transition period (~1 min) is not considered.

Line 127-129. "At this condition, the fractions of water-cluster ions are small, and the fragmentation of most VOCs product ions is not significant" This assumption is fundamental to the analysis presented in the remainder of the text, and the authors provide no evidence that this is true for their work. I would strongly suggest that they show some metric of the fragmentation and clustering that their instrument produced. A simple means would be to show the mass spectrum during a zero and calibration with known mixture (e.g. Apel Riemer standard) and quantify the ion(s) from each calibrant species.

Reply: We have added evidence of this assumption in the revised manuscript. The figure below shows the PTR-ToF-MS mass spectra from measurements of zero air and diluted gas standard with 5 ppb of various VOCs from a 16-component VOC gas standard (Apel Riemer Environmental Inc.). It can be seen that the fragmentation of most VOCs product ions is not significant, except monoterpene and ethanol, which are known to fragment significantly in PTR-MS. We included this graph in the SI of the revised manuscript.

At this condition, the fractions of water-cluster ions are small, and the fragmentation of most VOCs product ions is not significant (Figure S3) (de Gouw and Warneke, 2007;Yuan et al., 2017).

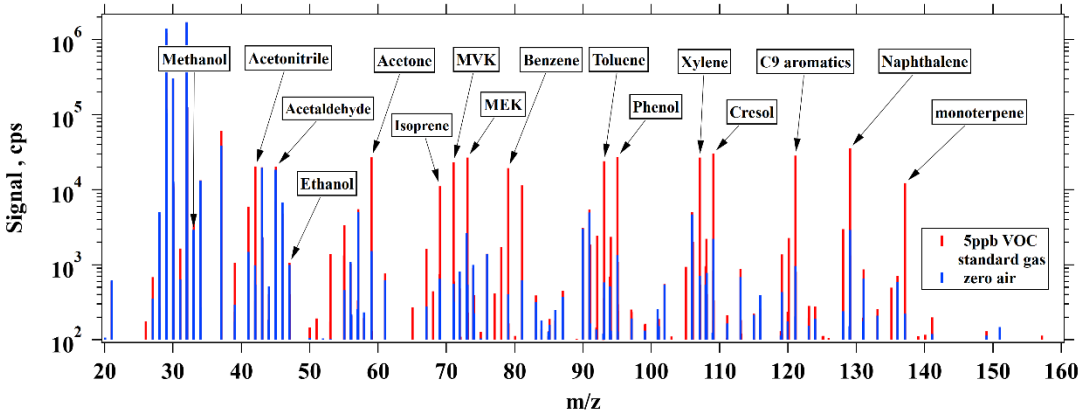

Figure S3. The mass spectra from measurements of zero air and diluted gas

standard with 5 ppb of various VOCs from a 16-component VOC gas standard.

Line 130-131 "The additional species measured by NO+ chemistry are discussed in a companion paper (Wang et al., 2020)." I did not find this listed in the reference section.

Reply: We have re-updated the cited reference:

The additional species measured by NO^+ chemistry are discussed in a companion paper (Wang et al., 2020a).

Line 153-154. "A total of 56 non-methane hydrocarbons (NMHCs) were measured us- ing a gas chromatography-mass spectrometer/flame ionization detector (GC-MS/FID) system." This description could use a few more details: at least sample frequency, sample collection time and volume.

Reply: We have added the description of GC-MS/FID in Section 2.

A total of 56 non-methane hydrocarbons (NMHCs) were measured using a gas chromatography-mass spectrometer/flame ionization detector (GC-MS/FID) system, coupled with a cryogen-free pre-concentration device (Wang et al., 2014). The system contains a two-channel sampling and GC column separation, able to measure C2-C5 hydrocarbons with the FID detection in one channel and measure C5-C12 hydrocarbons using MS detection in the other channel. The time resolution was 1 h, and ambient air was sampled during the first 5 minutes of each hour for both two channels with a flow of 300 ml/min. The uncertainties for VOC measurements by GC-MS/FID are estimated to be 15%-20% (Wang et al., 2014;Yuan et al., 2012a).

Line 158-160. "formaldehyde was also measured by a custom-built online instrument based on the Hantzsch reaction and absorption photometry from October 16 to Novem- ber 20, 2018." Is there any reference for this instrument? Can the authors provide LOD, sensitivity and/or accuracy for this measurement if not?

Reply: This instrument has been reported in the reference by Zhu et al. (2020). We have added this reference to provide the detailed information of custom-built online instrument based on the Hantzsch reaction and absorption photometry. The limit of detection of formaldehyde is 25 pptv for Hantzsch analyzer.

The sentences are changed to:

In addition to PTR-ToF-MS, formaldehyde was also measured by a custom-built online instrument based on the Hantzsch reaction and absorption photometry from October 16 to November 20, 2018. The detailed description of this instrument can be found in Zhu et al. (2020).

Line 164-165. "Formaldehyde measured by PTR-ToF-MS shows reasonable agree- ment with the Hantzsch formaldehyde instrument." The authors do not provide slopes for any of the plots in Figure S5 to allow the reader to evaluate. In particular, the slope of the formaldehyde inter-comparison looks to be approximately 2.5, which would not be a "reasonable agreement". The authors should discuss this discrepancy between the techniques, as the absolute mixing ratio of formaldehyde is important to understanding overall OH reactivity.

Reply: The fitted slope of formaldehyde measured by Hantzsch formaldehyde instrument versus PTR-ToF-MS is 2.45. Both Hantzsch formaldehyde instrument and PTR-ToF-MS were calibrated toward formaldehyde during the campaign. Measurements of formaldehyde by PTR-ToF-MS is challenging, due to the strong dependence of sensitivity as a function of humidity. In this study, we calibrated formaldehyde at different humidity to derive the humidity dependence curve for formaldehyde sensitivity (Figure S5 in the revised manuscript and Figure S4 in the original manuscript). Previous studies showed that formaldehyde measurements by PTR-MS by taking into account humidity dependence agree with other techniques within a factor of 2 (Warneke et al., 2011;Inomata et al., 2008;Vlasenko et al., 2010). The reason for the larger difference observed in this study is unknown, which might be related to calibration issues for either of the two instruments.

We agree with the reviewer that HCHO is important in OH reactivity. We used formaldehyde measured by PTR-ToF-MS to calculate OH reactivity in the manuscript, which contribute 2.9% of the measured OH reactivity. If using formaldehyde measured by Hantzsch formaldehyde instrument, formaldehyde contribution would be 7.1%, which is 4.2% higher. This would influence the values determined for OH reactivity from OVOCs and also missing reactivity in section 3.4. This result emphasizes the importance to accurately measure formaldehyde in analysis of OH reactivity. However, the discrepancy for formaldehyde measurements would not change the conclusions in this study.

We include this related information in the revised manuscript:

Formaldehyde measured by PTR-ToF-MS shows good correlation with the Hantzsch formaldehyde instrument (R=0.83), but concentrations measured by Hantzsch formaldehyde instrument are significantly higher than PTR-ToF-MS (slope=2.45). The reason for the large discrepancy is unknown. In the following discussions, formaldehyde measured by PTR-ToF-MS will be used.

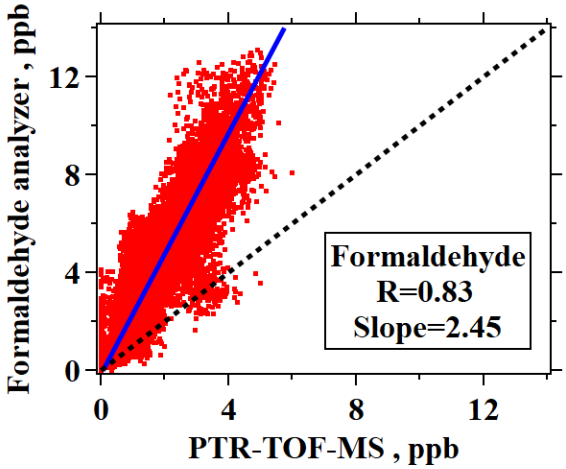

Line 191. "3.1 Characteristics of selected VOCs" Throughout this section, I found it difficult to understand which instrument was used to produce the data discussed. For example, line 194 ("Diurnal variations of hydrocarbons") is this NO+ PTR data or GC; line 203 ("The diurnal variation of aromatics") is this PTR or GC data?

Reply: We have stated in the caption of figure which instrument was used to produce the data discussed. The captions of Figure 1 and Figure 2 have been changed to:

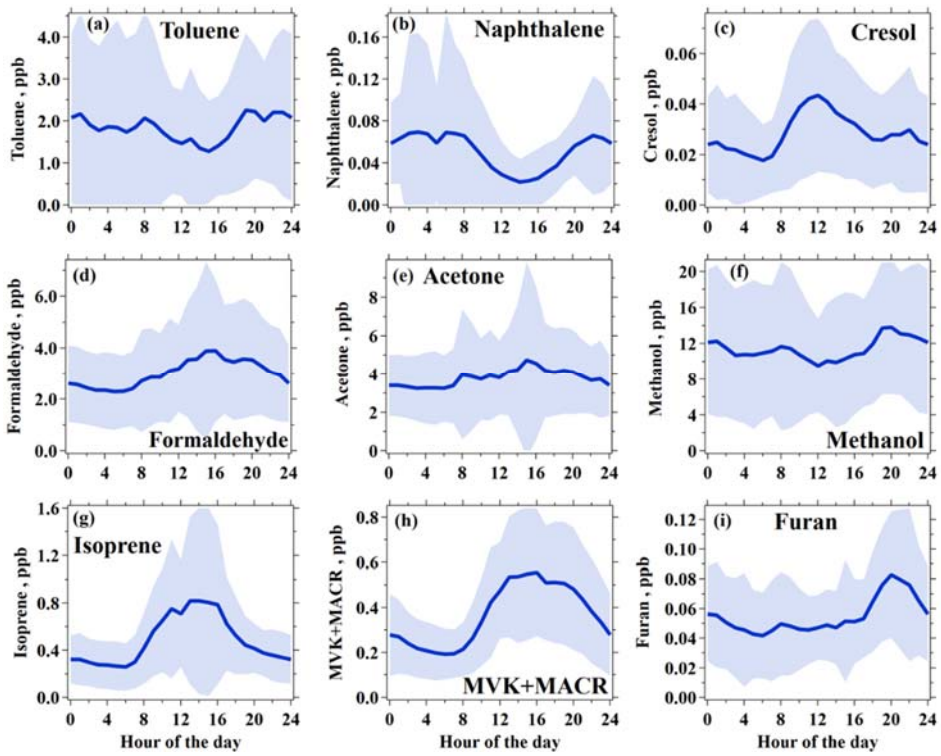

Figure 1. Diurnal variations of selected VOCs measured by PTR-ToF-MS during the campaign. Blue lines and shaded areas represent averages and standard deviations, respectively.

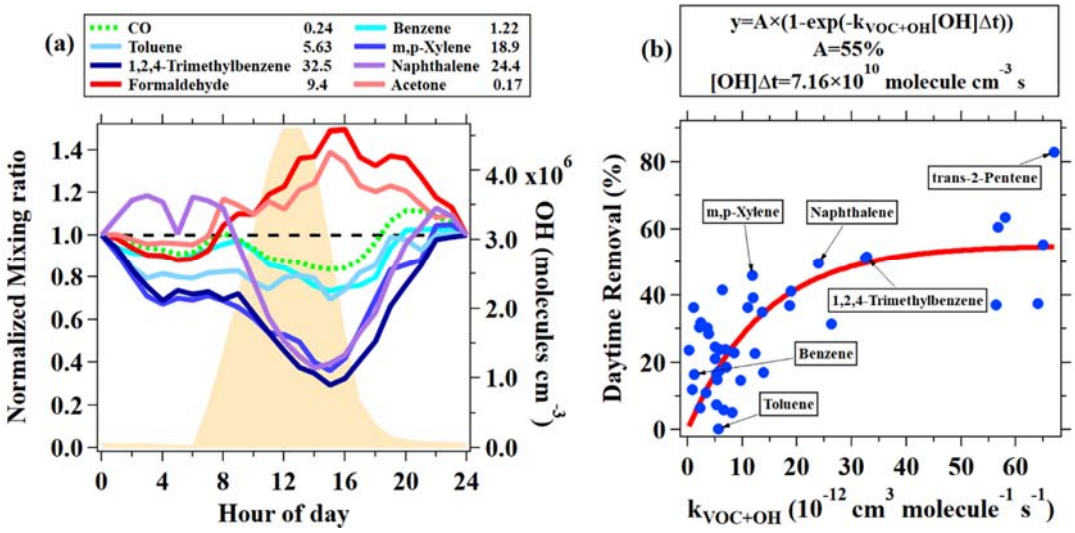

Figure 2. (a) Normalized diurnal variations of CO, five aromatic hydrocarbons (benzene, toluene, m,p-xylene, 1,2,4-trimethylbenzene measured by GC-MS/FID and naphthalene measured by PTR-ToF-MS) and two OVOCs (formaldehyde and acetone measured by PTR-ToF-MS). The data are normalized to midnight values. The rate coefficients for the reactions with OH radicals are shown in the legend (in units of 10^{-12} cm^3 $molecule^{-1}$ s^{-1}). The orange shaded area indicates the average diurnal variation of simulated OH by an observation-constrained box model. (b)

Daytime removal fractions of all hydrocarbons measured by GC-MS/FID and also naphthalene by PTR-ToF-MS as a function of their rate constants with OH. The daytime removal fractions for VOCs species were calculated from the concentration ratio between measurement at 14:00 and at 6:00-8:00.

Line 215-217. "The estimated OH concentration is in good agreement with simulated average OH concentration during the same period using an observation-constrained box model" The authors should provide further description and/or reference to this model.

Reply: We thanks the reviewer for the comment. We added the description to the box model in Section 3.1 of the revised manuscript:

The estimated OH concentration is in good agreement with simulated average OH concentration during the same period using an observation-constrained box model (3.4×10^6 molecule cm^{-3}) (Figure 2a), which is constrained using measurements of trace gases, VOCs, photolysis frequencies and meteorological parameters with Master Chemical Mechanism (MCM) v3.3.1 as the chemical mechanism (Wang et al., 2020b). The box model is run using the Framework for 0-D Atmospheric Modeling (F0AM) v3.1 (Wolfe et al., 2016).

Line 260. "A peak list with more than 1700 ions was used to perform high-resolution peak fittings" Please cite the software used for peak fitting.

Reply: We have added the software used for peak fitting and the sentence is changed to:

A peak list with more than 1700 ions was used to perform high-resolution peak fittings by Tofware (version 3.0.3; Tofwerk AG, Switzerland). More detailed description of Tofware can be found in elsewhere (Stark et al., 2015).

Line 268-269. "We also tried the method proposed in Sekimoto et al. (2017), but no clear relationship between calibration factors and their capture kinetic rate constants was derived." This is a surprising result. Do the authors understand why no relationship was found?

Reply: We re-checked the relationship between the sensitivity and rate constants for proton-transfer reactions of H_3O^+ with VOCs. We found that the reason for the lack of linearity in the original manuscript: we used the thermal rate constant in the original

manuscript, while the kinetic rate constants should be used. The kinetic rate constants consider the much higher energetic collisions that is controlled by both temperature in the drift tube and also the E/N ratio (120 Td) (Cappellin et al., 2012;Sekimoto et al., 2017). After using the kinetic rate constant of each VOC, we obtained the linear relationship between the sensitivity and kinetic rate constant for proton-transfer reactions of H_3O^+, and used this linearity to re-calculate the concentration of uncalibrated species.

As discussed in section 2.2, a total of 31 VOCs species were calibrated using either gas cylinders or liquid standards. For other VOCs, we used the method proposed in Sekimoto et al. (2017) to determine the relationship between VOCs sensitivity and kinetic rate constants for proton-transfer reactions of H_3O^+ with VOCs (detailed discussions in the SI). As shown in Figure 3, a clear linear relationship was obtained. The fitted line in Figure 3 is used to determine sensitivities of the uncalibrated species. Following the discussions in Sekimoto et al. (2017), uncertainties of the concentrations for uncalibrated species are around 50%.

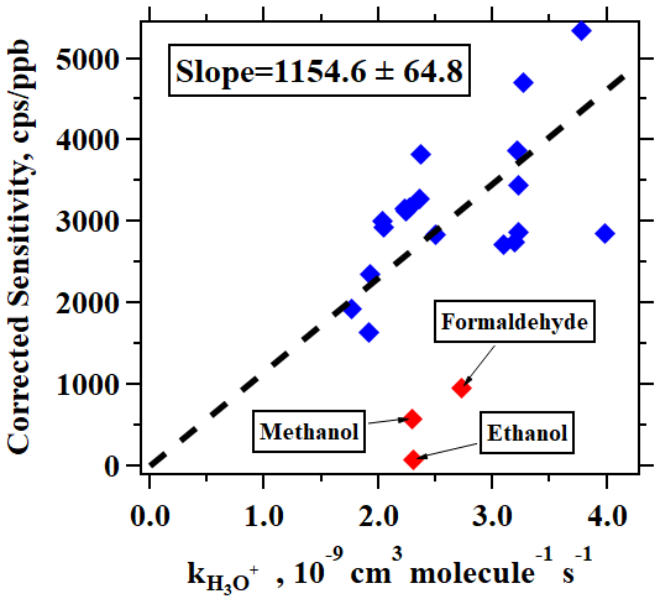

Figure 3. Corrected sensitivities as a function of kinetic rate constants for proton-transfer reactions of H_3O^+ with VOCs. The dashed line indicates the fitted line for blue points. The red points are not used, as these compounds (formaldehyde, methanol, ethanol) are known to have lower sensitivities.

Line 270-271. "Therefore, we used the average calibration factor of 4170 cps/ppb

to quantify those species without external calibration measured by PTR-ToF-MS." The authors should estimate the uncertainty of the cal factor and propagate that uncertainty throughout the ensuing discussion. Also, Table S1 shows that organic acids and N-containing species typically had sensitivities significantly lower than 4000 cps/ppb. Does this imply that a single calibration factor is appropriate across all of the binned formulas discussed later?

Reply: As shown in the response of the above comment, we re-checked the relationship between the sensitivity and kinetic rate constant for proton-transfer reactions of H_3O^+. In the revised manuscript, we obtained the linear relationship between the sensitivity and kinetic rate constant for proton-transfer reactions of H_3O^+ as shown in Sekimoto et al. (2017), and used this linearity to recalculate the concentration of uncalibrated species. Following the discussions in Sekimoto et al. (2017), the uncertainties of determined concentrations of uncalibrated species are around 50%. The effects of the uncertainties in concentrations of uncalibrated species are also discussed in section 3.2 and 3.4.

As discussed in section 2.2, a total of 31 VOCs species were calibrated using either gas cylinders or liquid standards. For other VOCs, we used the method proposed in Sekimoto et al. (2017) to determine the relationship between VOCs sensitivity and kinetic rate constants for proton-transfer reactions of H_3O^+ with VOCs (detailed discussions in the SI). As shown in Figure 3, a clear linear relationship was obtained. The fitted line in Figure 3 is used to determine sensitivities of the uncalibrated species. Following the discussions in Sekimoto et al. (2017), uncertainties of the concentrations for uncalibrated species are around 50%.

Adding up these contributions, it significantly narrows the gap between the measured and calculated OH reactivity, leaving only 11% of OH reactivity as "missing" during the campaign. Considering the large uncertainties for both concentrations (~50%) and rate constants of the uncalibrated species (on the order of 100%), the missing reactivity can ranged in 0%-19%. Nevertheless, the determined missing reactivity would be well below the estimated uncertainty (20%) for the OH reactivity measurements by the CRM method, indicating that gap between measured and calculated reactivity can be significantly narrowed after taking into account all of the species by PTR-ToF-MS.

Line 273-274 "We divided the VOCs measured by PTR-ToF-MS into groups according to the oxygen atoms in the formula" This analysis assumes that fragmentation and clustering are insignificant contributors to the mass spectra of ambient air. As noted above, the authors should defend this assumption and/or provide some measure of the uncertainty of their assumption.

Reply: We have added evidence of this assumption in the revised manuscript. The figure below shows the PTR-ToF-MS mass spectra from measurements of zero air and diluted gas standard with 5 ppb of various VOCs from a 16-component VOC gas standard (Apel Riemer Environmental Inc.). It can be seen that the fragmentation of most VOCs product ions is not significant, except monoterpene and ethanol, which are known to fragment significantly in PTR-MS. We included this graph in the SI of the revised manuscript.

At this condition, the fractions of water-cluster ions are small, and the fragmentation of most VOCs product ions is not significant (Figure S3) (de Gouw and Warneke, 2007;Yuan et al., 2017).

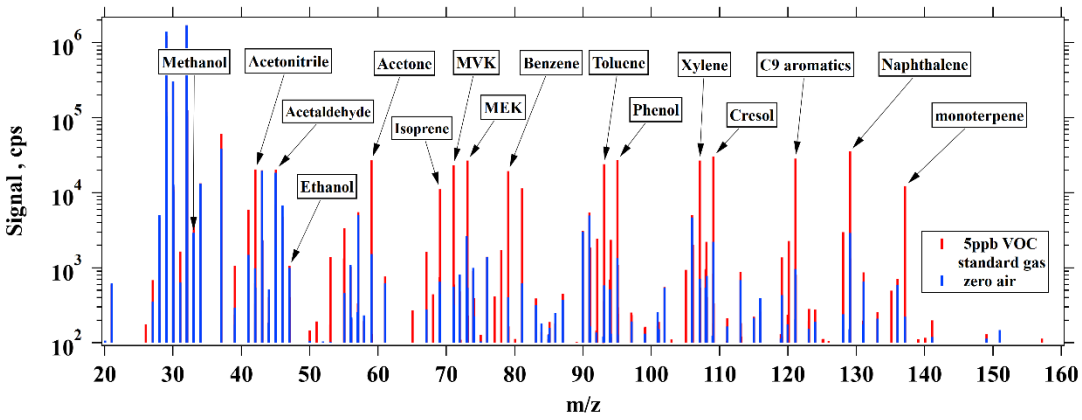

Figure S3. The mass spectra from measurements of zero air and diluted gas standard with 5 ppb of various VOCs from a 16-component VOC gas standard.

Line 284 "The low contributions from OVOCs with three or more oxygen atoms are different from the concurrent observations of iodide ToF-CIMS during the campaign" This is the only mention of the IâA˘T˘ CIMS instrument that I can find in the manuscript. The authors should provide some description of this instrument in Section 2, especially the inlet used by the I-CIMS as that would be relevant to the discussion here. The language in this comparison of relative abundance of more-highly oxidized OVOCs implies that the PTR method is less sensitive to these species due to losses. The authors should also consider that the I-CIMS technique is relatively

insensitive to less oxidized OVOCs.

Reply: This description are added in the Section 2 of the revised manuscript.

An iodide-adduct time-of-flight chemical ionization mass spectrometer (ToF-CIMS) (Aerodyne Research, Inc.) coupled with a Filter Inlet for Gases and Aerosols (FIGAERO) inlet was used for measuring oxygenated VOCs in ambient air (Wang et al., 2020b). The Filter Inlet for Gases and Aerosols (FIGAERO) sampling assembly switches the air flow between two inlets, one designed for gases and the other for chemicals thermally desorbed from aerosols, which provides the online measurements of species from both gas-phase and particle-phase (Thornton et al., 2020;Lopez-Hilfiker et al., 2014).

Line 308-309. "If only considering the six common OVOCs measured by PTR-MS, i.e. formaldehyde, acetaldehyde, methanol, acetone, MEK and MVK+MACR". Where do the authors get this list of OVOCs? They should cite the reference, or the survey of references used for this.

Reply: Thanks for the valuable suggestion. We have added the corresponding references in the revised manuscript:

If only considering the six common OVOCs measured by PTR-MS, i.e. formaldehyde, acetaldehyde, methanol, acetone, MEK and MVK+MACR (de Gouw et al., 2003;de Gouw and Warneke, 2007), the OVOCs fraction in total VOCs would be only 39%.

Line 313. Source analysis of OVOCs. This section describes an analysis method that attributes OVOC sources to primary anthropogenic, secondary formation, biogenic and background. An implicit assumption here is that a single anthropogenic tracer (acetylene or CO) can characterize all primary anthropogenic emissions. That is, primary anthro emissions are homogeneous for the sampling site. The authors should state this in the text.

Reply: Thank you for pointing this out. CO and acetylene has proven to be a good tracer for urban emissions, and many literature studies have reported the use of CO and acetylene as anthropogenic tracers in urban (de Gouw et al., 2008;Yuan et al., 2012b), so we use acetylene or CO as a anthropogenic tracer, and we have already stated this in Section 3.3: The photochemical age-based parameterization method for source analysis of OVOCs is based on the following assumptions: (1) the amount of each OVOCs

emitted is proportional to an inert tracer (e.g. CO and acetylene C_2H_2) (Yuan et al., 2012b;de Gouw et al., 2005);

Line 377-378. "An effective OH rate constant of 2×10-^{11} cm3 molecule-1 s-1 was applied for different ion groups." It is not clear how this value was determined to be appropriate. Please provide some rationale for using this value.

Reply: The OH rate constants are needed for the source analysis of different OVOCs ion groups. However, this parameter is not possible to obtain, unless the OH rate constants for each ion is known. To approximate the effective OH rate constant, we calculate the median (2.0×10^{-11} cm^3 $molecule^{-1}$ s^{-1}) for the OH rate constants for all OVOCs ions that are listed in Table S4 in the revised manuscript. As the result, we use 2.0×10^{-11} cm^3 $molecule^{-1}$ s^{-1} as the best estimate for the effective OH rate constant for OVOCs ion groups.

We included this informaiton in the revised manuscript:

An effective OH rate constant of 2.0×10^{-11} cm^3 $molecule^{-1}$ s^{-1} (the median for all OVOCs ions in Table S4) was applied for different ion groups.

Line 394. "VOCs reactivity can visually and effectively characterize" It's not clear what the authors mean by "visually" here.

Reply: This sentence is changed in the revised manuscript:

VOCs reactivity can effectively characterize the contributions of various VOCs to atmospheric chemical reactions that are related to the formation of secondary pollutants.

Line 809. Figure 2. This appears to be GC data, based upon the species shown (e.g. isomers). The authors should state explicitly if this is the case. Also, In Figure 2b, the labeling of some dots in the figure seems arbitrary. Consider limiting labels to those species discussed in the main text or significant outliers, e.g. the point in the top right corner, which seems a significant, and perhaps interesting, outlier to the overall good fit of the data.

Reply: Thanks for the suggestion. In Figure 2 a, benzene, toluene, m,p-xylene and 1,2,4-trimethylbenzene are measured by GC-MS/FID, and naphthalene, formaldehyde and acetone are measured by PTR-ToF-MS, which has been illustrated in the caption of Figure 2a. Following the suggestion from the reviewer, the species shown in Figure

2a and significant outliers are marked as labels in Figure 2b.

The caption of Figure 2 has been changed to:

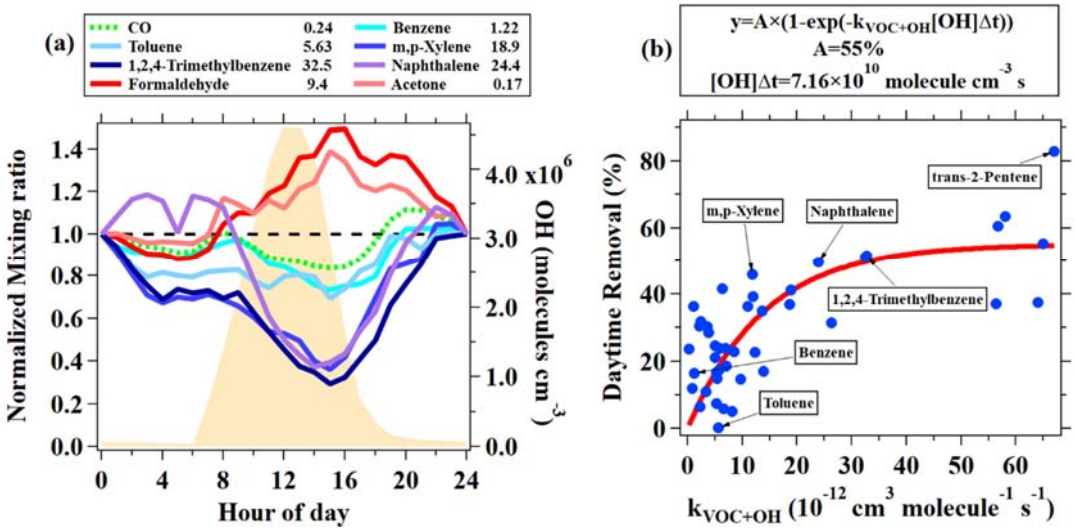

Figure 2. (a) Normalized diurnal variations of CO, five aromatic hydrocarbons (benzene, toluene, m,p-xylene, 1,2,4-trimethylbenzene measured by GC-MS/FID and naphthalene measured by PTR-ToF-MS) and two OVOCs (formaldehyde and acetone measured by PTR-ToF-MS). The data are normalized to midnight values. The rate coefficients for the reactions with OH radicals are shown in the legend (in units of 10^{-12} cm^3 $molecule^{-1}$ s^{-1}). The orange shaded area indicates the average diurnal variation of simulated OH by an observation-constrained box model. (b) Daytime removal fractions of all hydrocarbons measured by GC-MS/FID and also naphthalene by PTR-ToF-MS as a function of their rate constants with OH. The daytime removal fractions for VOCs species were calculated from the concentration ratio between measurement at 14:00 and at 6:00-8:00.

Line 820. Figure 3. I found this figure difficult to interpret as the colors are similar and the figure is highly detailed. My suggestion: could the authors reformat as a stacked- axis plot, with the five categories of ions on their own y-axis?

Reply: We thank the reviewer for the comment. Figure 3 shows the average mass spectra measured by PTR-ToF-MS during the campaign. Here, we divide the ions in the mass spectra into five different ion categories, following the procedures in many previous online mass spectrometry studies (Koss et al., 2017;Stockwell et al., 2015;Zhang et al., 2018). We tried to modify the graph according to the suggestion from the reviewer by placing five categories of ions on their own y-axis and reformatted as a stacked axis plot. However, we found the concentration from different categories

cannot be compared easily. As the result, we decide to keep plotting the graph this way. Nevertheless, we made the graph taller, which should be easier to read sticks in the graph.

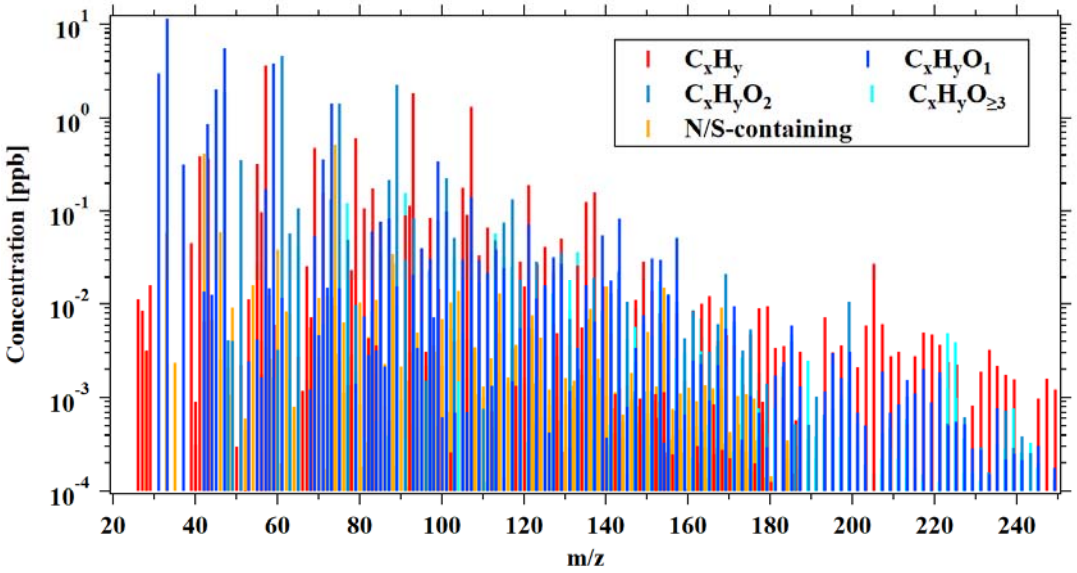

Figure 3. Average mass spectra obtained by PTR-ToF-MS from ambient measurement during the campaign. The different ion categories are detailedly discussed in the text.

Line 823. Figure 4. The pie charts in (a) and (c) don't seem to match the diurnal trends in (b) and (d), respectively. The mixing ratios shown in (b) and (d) would imply different sizes of the wedges that make up each pie chart than are shown. Perhaps I am mis-interpreting what is presented? Supplement, Table S4. I found this table to be especially problematic, as the authors provide an enormous list of ions with associated OH reactivities. Since the authors never attribute a parent molecule to these ions, this makes these attributions impossible to evaluate. For comparison, Koss et al. (2018) provides a similar table in their supplemental materials, but also provides a master table that links each ion with a suspected or confirmed parent. The authors should revise this table to give a suspected / confirmed parent in each case.

Reply: We thank the reviewer for the comment. In order to demonstrate the diurnal variations of different categories of VOCs clearly on the same y-axis in Figure 4b and 4d, concentrations of some categories are plotted by multiplying scale factors, which are explicitly indicated in the figure legend. For example, OVOC concentrations shown in Figure 4d are the results of multiplying a factor of 0.1 of the measured concentrations.

In terms of Table S4, we added our attributions of the most possible compounds

to the ions, based on previous review and studies (Yuan et al., 2017;Koss et al., 2018).

Table S4 in SI has been changed to:

Table S4. The average concentrations of VOCs measured by PTR-ToF-MS and their OH rate constants, which were used for calculating OH reactivity.

Ion exact mass (Th)	Ion formula	Compound	Average concentration (ppb)	OH rate constant (10^{-12} cm^3 $molecule^{-1}$ s^{-1})	Source of OH rate constants
Common OVOCs					
30.0178	CH_2O	Formaldehyde	2.991±2.059	9.4	Atkinson 2003[21]
32.0335	CH_4O	Methanol	11.43±7.612	0.8	Atkinson 2003
44.0335	C_2H_4O	Acetaldehyde	2.027±1.292	15.0	Atkinson 2003
56.0335	C_3H_4O	Acrolein	0.173±0.102	20.0	Gilman 2015
58.0491	C_3H_6O	Acetone	3.798±2.508	0.2	Atkinson 2003
70.0491	C_4H_6O	MVK+MACR	0.362±0.249	24.8	Koss 2018[32]
72.0648	C_4H_8O	MEK	1.420±1.309	5.5	Koss 2018
86.0804	$C_5H_{10}O$	Pentanones	0.085±0.049	7.9	Atkinson 2003
100.096	$C_6H_{12}O$	Hexanones	0.101±0.091	18.6	Koss 2018
NMHCs					
184.36	$C_{13}H_{28}$	Tridecane#	0.066±0.060	15.3	Atkinson 2003
198.39	$C_{14}H_{30}$	Tetradecane#	0.050±0.047	16.7	Atkinson 2003
212.41	$C_{15}H_{32}$	Pentadecane#	0.045±0.042	18.1	Atkinson 2003
226.44	$C_{16}H_{34}$	Hexadecane#	0.036±0.033	19.4	Atkinson 2003
240.46	$C_{17}H_{36}$	Heptadecane#	0.021±0.020	20.7	Atkinson 2003
254.49	$C_{18}H_{38}$	Octadecane#	0.013±0.014	21.9	Atkinson 2003

268.52	$C_{19}H_{40}$	Nonadecane[#]	0.005±0.009	23	Atkinson 2003
282.54	$C_{20}H_{42}$	Eicosane[#]	0.0007±0.004	24	Atkinson 2003
40.038	C_3H_4	1,2-Propadiene	0.758±0.971	0.695	Pfannerstill 2019
66.054	C_5H_6	Cyclopentadiene	0.038±0.029	92.0	Gilman 2015
82.085	C_6H_{10}	Methylcyclopentane	0.225±0.158	6.97	Atkinson 2003
84.101	C_6H_{12}	Hexene isomers	0.098±0.078	37	Atkinson 2003
94.085	C_7H_{10}	Terpene fragment	0.047±0.041	46.8	Pfannerstill 2019
96.101	C_7H_{12}	C7 cycloalkanes	0.103±0.073	9.64	Atkinson 2003
102.054	C_8H_6	Phenylacetylene	0.005±0.004	1.0	Gilman 2015
108.101	C_8H_{12}	Terpene fragment	0.036±0.041	107	Pfannerstill 2019
110.116	C_8H_{14}	C8 cycloalkanes	0.075±0.055	9.64	Atkinson 2003
116.07	C_9H_8	Indene	0.004±0.009	78.0	Atkinson 2003
118.086	C_9H_{10}	Indane	0.032±0.031	50.4	Atkinson 2003
128.07	$C_{10}H_8$	Naphthalene	0.052±0.061	23.0	Atkinson 2003
130.086	$C_{10}H_{10}$	Methyl indene	0.004±0.005	28.5	Koss 2018
132.101	$C_{10}H_{12}$	Tetrahydronaphthalene	0.028±0.026	33.0	Koss 2018
134.117	$C_{10}H_{14}$	C10 aromatics	0.133±0.141	9.5	Koss 2018
136.132	$C_{10}H_{16}$	Monoterpenes	0.161±0.245	162.8	Koss 2018
142.086	$C_{11}H_{10}$	Methyl naphthalene	0.015±0.017	50.0	Koss 2018
144.101	$C_{11}H_{12}$	C11 6-DBE	0.001±0.003	78.0	Koss 2018
146.116	$C_{11}H_{14}$	aromatic fragment	0.011±0.015	58	Pfannerstill 2019
148.132	$C_{11}H_{16}$	C11 aromatics	0.030±0.031	50.0	Koss 2018

152.07	$C_{12}H_8$	Acenaphtylene	0.001±0.003	15.1	Koss 2018
156.101	$C_{12}H_{12}$	C2 naphthalene	0.008±0.009	60.0	Koss 2018
160.132	$C_{12}H_{16}$	aromatic fragment	0.009±0.012	58	Pfannerstill 2019
162.148	$C_{12}H_{18}$	C12 aromatics	0.010±0.010	113.0	Koss 2018
174.148	$C_{13}H_{18}$	C13 5-DBE	0.005±0.008	38.5	Pfannerstill 2019
176.164	$C_{13}H_{20}$	C13 aromatics	0.009±0.010	113.0	Koss 2018
Novel OVOCs					
46.0128	CH_2O_2	Formic acid	1.880±3.155	0.4	Koss 2018
46.0491	C_2H_6O	Ethanol	5.634±5.192	3.2	Atkinson 2003
48.0284	CH_4O_2	Methane diol	0.005±0.003	7.0	Koss 2018
54.0178	C_3H_2O	Propynal	0.005±0.057	20.0	Koss 2018
58.0128	$C_2H_2O_2$	Glyoxal	0.001±0.002	11.0	Atkinson 2003
60.0284	$C_2H_4O_2$	Acetic acid	4.618±4.681	3.7	Koss 2018
62.044	$C_2H_6O_2$	Ethane diol	0.070±0.068	14.5	Pfannerstill 2019
64.023	CH_4O_3	formic acid water cluster	0.039±0.048	7.1	Pfannerstill 2019
68.0335	C_4H_4O	Furan	0.055±0.036	40.0	Gilman 2015
70.0128	$C_3H_2O_2$	Propiolic acid	0.008±0.010	26.0	Koss 2018
72.0284	$C_3H_4O_2$	Methyl glyoxal	0.143±0.093	21.1	Koss 2018
74.0441	$C_3H_6O_2$	Propanoic acid	1.438±2.188	2.2	Koss 2018
76.059	$C_3H_8O_2$	Propane diols	0.053±0.046	16.2	Pfannerstill 2019
80.0335	C_5H_4O	Cyclopentadiene ketone	0.006±0.005	20.0	Gilman 2015 2-methylfuran

82.0491	C_5H_6O	Methyl furan	0.081±0.063	37.1	Gilman 2015 cyclopentenone
84.0284	$C_4H_4O_2$	Furanone	0.036±0.025	44.5	Gilman 2015
84.0648	C_5H_8O	C5 ketones	0.060±0.043	11.5	Atkinson 2003, NIST Database
86.0441	$C_4H_6O_2$	2,3-Butanedione	±	0.8	Gilman 2015, NIST Database
88.0233	$C_3H_4O_3$	Pyruvic acid	0.009±0.026	0.1	Gilman 2015
88.0597	$C_4H_8O_2$	Methyl propanoate	2.273±2.367	0.9	Koss 2018
94.0491	C_6H_6O	Phenol	0.039±0.030	28.0	Gilman 2015
96.0284	$C_5H_4O_2$	Furfural	0.023±0.020	35.6	Gilman 2015
96.0648	C_6H_8O	Dimethyl or ethyl furan	0.039±0.025	132.0	Gilman 2015 25dimethylfuran
98.0441	$C_5H_6O_2$	Methyl furanone	0.050±0.033	13.6	Koss 2018
98.0804	$C_6H_{10}O$	Hexenones	0.262±0.278	6.4	Atkinson 2003 cyclohexanone
100.023	$C_4H_4O_3$	Dihydro furandione	0.040±0.062	20.0	Koss 2018
100.06	$C_5H_8O_2$	Methyl methacrylate	0.248±0.163	30.3	Gilman 2015
102.039	$C_4H_6O_3$	Acetic anhydride	0.026±0.020	43.0	Koss 2018
102.0753	$C_5H_{10}O_2$	Pentanoic acids	0.058±0.055	8.71	Pfannerstill 2019
106.049	C_7H_6O	Benzaldehyde	0.104±0.099	12.0	Atkinson 2003
108.028	$C_6H_4O_2$	Benzoquinone	0.016±0.015	4.6	NIST Database
108.065	C_7H_8O	Cresols	0.028±0.023	26.2	NIST Database
110.044	$C_6H_6O_2$	Methyl furfural	0.022±0.017	80.1	Koss 2018
110.08	$C_7H_{10}O$	C3 furan	0.026±0.017	23.3	Koss 2018
112.023	$C_5H_4O_3$	Methylfurandione	0.052±0.049	49.0	Koss 2018
112.06	$C_6H_8O_2$	Dimethylfuranone	0.043±0.031	57.0	Koss 2018

112.096	$C_7H_{12}O$	Ethyl cyclopentanone	0.029±0.028	10.0	NIST Database cycloheptanone
114.039	$C_5H_6O_3$	C5 3-oxy 3DBE	0.029±0.024	100.0	Koss 2018
114.075	$C_6H_{10}O_2$	C6 diketone isomers	0.075±0.057	20.0	Koss 2018
114.112	$C_7H_{14}O$	heptanal	0.019±0.013	21.4	Atkinson 2003
116.055	$C_5H_8O_3$	C5 3-oxy 2-DBE isomers	0.022±0.017	5.0	Koss 2018
116.091	$C_6H_{12}O_2$	Butyl ester acetic acid	0.135±0.136	6.0	NIST Database
118.049	C_8H_6O	Benzofuran	0.006±0.007	37.0	NIST Database
120.065	C_8H_8O	Tolualdehyde	0.056±0.044	16.0	Atkinson 2003 average tolualdehydes
122.044	$C_7H_6O_2$	Salicyladehyde	0.022±0.023	38.0	Koss 2018
122.08	$C_8H_{10}O$	Ethylphenol	0.012±0.012	46.6	Koss 2018
124.023	$C_6H_4O_3$	Hydroxy benzoquiunone	0.002±0.002	4.6	Koss 2018
124.06	$C_7H_8O_2$	guaiacol	0.014±0.011	75.0	NIST Database
124.096	$C_8H_{12}O$	C4 furan	0.018±0.010	40.4	Pfannerstill 2019
126.039	$C_6H_6O_3$	Hydroxymethyl furfural	0.012±0.009	100.0	Koss 2018
126.111	$C_8H_{14}O$	Cyclooctanone	0.024±0.027	98.8	Pfannerstill 2019
128.055	$C_6H_8O_3$	Methyl hydroxy dihydrofurfural	0.023±0.019	132.0	Koss 2018
128.127	$C_8H_{16}O$	Octanal	0.021±0.015	11	Pfannerstill 2019
132.065	C_9H_8O	Methyl benzofurans	0.004±0.005	37.0	Gilman 2015
134.08	$C_9H_{10}O$	3-methylacetophenone	0.012±0.010	4.5	NIST Database
136.06	$C_8H_8O_2$	Methyl benzoic acid	0.019±0.018	12.0	Koss 2018

138.075	$C_8H_{10}O_2$	Creosol	0.008±0.007	100.0	NIST Database
140.127	$C_9H_{16}O$	C9 carbonyl +1DBE	0.014±0.010	43.5	Pfannerstill 2019
144.05	$C_6H_8O_4$	C6 diacid +1DBE	0.004±0.003	4.6	Koss 2018
144.065	$C_{10}H_8O$	Ethenyl benzofuran	0.001±0.002	37.0	Koss 2018
146.08	$C_{10}H_{10}O$	Dimethylbenzofuran	0.004±0.004	37.0	Koss 2018
148.096	$C_{10}H_{12}O$	Methyl chavicol (estragole)	0.008±0.007	50.0	NIST Database: 1-methoxy-4-(2-propenyl) benzene
150.075	$C_9H_{10}O_2$	Vinyl guaiacol	0.004±0.004	100.0	Koss 2018
152.055	$C_8H_8O_3$	Vanillin	0.016±0.010	85.0	Koss 2018
152.127	$C_{10}H_{16}O$	Camphor	0.028±0.018	4.3	Atkinson 2003
154.07	$C_8H_{10}O_3$	Syringol	0.004±0.004	100.0	Koss 2018
154.143	$C_{10}H_{18}O$	Linalool	0.012±0.009	25.0	NIST Database Fenchol, Borneol
156.159	$C_{10}H_{20}O$	Decanal	0.051±0.066	13.0	Atkinson 2003 2-decanone
164.091	$C_{10}H_{12}O_2$	Eugenol	0.003±0.003	100.0	Koss 2018
N/S-containing species					
27.0182	HCN	HCN	0.003±0.002	0.0	Cicerone 1983
33.995	H_2S	Hydrogen sulfide	0.005±0.004	4.6	NIST database
41.0338	C_2H_3N	Acetonitrile	0.412±2.258	0.02	Gilman 2015
43.0495	C_2H_5N	Etheneamine	0.010±0.011	0.2	Koss 2018
45.0287	CH_3NO	Formamide	0.046±0.092	1.5	NIST database: CH2=NOH
45.0651	C_2H_7N	Ethylamine	0.004±0.007	45.5	Koss 2018
48.0106	CH_4S	Methane thiol	0.012±0.014	33.0	NIST database
53.0338	C_3H_3N	Acrylonitrile	0.011±0.007	4.0	Gilman 2015

55.0495	C_3H_5N	Propane nitrile	0.003±0.004	0.3	Gilman 2015
57.0287	C_2H_3NO	Methyl isocyanate	0.011±0.007	0.1	Koss 2018
57.0651	C_3H_7N	Propene amine	0.004±0.005	15.0	Koss 2018
59.0444	C_2H_5NO	Acetamide	0.029±0.055	8.6	NIST database
61.0237	CH_3NO_2	Nitromethane	0.006±0.006	0.3	Gilman 2015
62.0263	C_2H_6S	Dimethyl sulfide	0.010±0.012	6.0	NIST database
65.0338	C_4H_3N	Cyanoallene isomers	0.001±0.007	4.0	Koss 2018
67.0495	C_4H_5N	Pyrrole	0.006±0.007	111.4	Gilman 2015
69.0651	C_4H_7N	Dihydropyrrole	0.008±0.004	7.7	Koss 2018
71.0808	C_4H_9N	Butene amines	0.001±0.001	25.0	Koss 2018
73.0237	$C_2H_3NO_2$	Nitroethene	0.001±0.007	1.2	NIST Database
73.06	C_3H_7NO	C3 amides	0.350±0.616	12.5	Pfannerstill 2019
75.0393	$C_2H_5NO_2$	Nitroethane	0.005±0.004	0.1	NIST Database
77.0008	CH_3NOS	Sulfinyl methanamine	0.001±0.001	0.2	Koss 2018
79.0495	C_5H_5N	Pyridine	0.010±0.006	5.6	Koss 2018
81.0651	C_5H_7N	Methyl pyrrole	0.004±0.006	62.7	Gilman 2015
83.0808	C_5H_9N	C5 nitrile	0.007±0.003	0.5	Koss 2018
89.055	$C_3H_7NO_2$	Nitropropanes	0.001±0.002	1.2	NIST Database
93.0287	C_5H_3NO	2-furancarbonitrile	0.000±0.001	40.0	Koss 2018
93.0651	C_6H_7N	2-methyl pyridine	0.006±0.005	2.6	NIST Database methylpyridines average
93.9984	$C_2H_6S_2$	Dimethyl disulfide	0.004±0.005	230.0	NIST Database

95.0444	C_5H_5NO	4-Pyridinol	0.001±0.001	0.5	Koss 2018
95.0808	C_6H_9N	1-ethyl pyrrole	0.001±0.001	145.0	Koss 2018
97.0964	$C_6H_{11}N$	4-methylpentanenitrile	0.002±0.001	5.0	Koss 2018
103.049	C_7H_5N	Benzonitrile	0.008±0.006	1.0	Gilman 2015
105.065	C_7H_7N	Vinylpyridine	0.001±0.003	57.0	NIST Database
107.044	C_6H_5NO	nitrosobenzene or pyridine aldehyde	0.002±0.002	12.0	Koss 2018
107.081	C_7H_9N	Toluidine	0.004±0.005	3.2	NIST Database
109.096	$C_7H_{11}N$	C7 acrylonitrile	0.001±0.001	89.4	Koss 2018
111.039	$C_5H_5NO_2$	Dihydroxy pyridine	0.002±0.001	10.3	Koss 2018
113.019	$C_4H_3NO_3$	Nitrofuran	0.005±0.005	40.0	Koss 2018
117.05	$C_4H_7NO_3$	Butene nitrates	0.004±0.005	50.8	Koss 2018
117.065	C_8H_7N	Indole	0.003±0.003	1.2	Koss 2018
119.081	C_8H_9N	Dihydro pyridine	0.000±0.001	0.5	Koss 2018
123.039	$C_6H_5NO_2$	Nitrobenzene	0.003±0.005	0.1	NIST Database
125.128	$C_8H_{15}N$	C8 nitriles	0.000±0.001	8.0	Koss 2018
131.081	C_9H_9N	Methyl indole	0.001±0.001	5.6	Koss 2018
137.055	$C_7H_7NO_2$	Nitrotoluene	0.002±0.002	0.1	Koss 2018
149.127	$C_{10}H_{15}N$	C10 aromatic amines	0.000±0.001	148	Pfannerstill 2019

496

Reference：

Atkinson, R., and Arey, J.: Atmospheric Degradation of Volatile Organic Compounds, Chemical Reviews, 103, 4605-4638, 10.1021/cr0206420, 2003.

Atkinson, R., Baulch, D. L., Cox, R. A., Crowley, J. N., Hampson, R. F., Hynes, R. G., Jenkin, M. E., Rossi, M. J., and Troe, J.: Evaluated kinetic and photochemical data for atmospheric chemistry: Volume I - gas phase reactions of Ox, HOx, NOx and SOx species, Atmospheric Chemistry and Physics, 4, 1461-1738, 10.5194/acp-4-1461-2004, 2004.

Atkinson, R., Baulch, D. L., Cox, R. A., Crowley, J. N., Hampson, R. F., Hynes, R. G., Jenkin, M. E., Rossi, M. J., Troe, J., and Subcommittee, I.: Evaluated kinetic and photochemical data for atmospheric chemistry: Volume II – gas phase reactions of organic species, Atmospheric Chemistry and Physics, 6, 3625-4055, 10.5194/acp-6-3625-2006, 2006.

Cappellin, L., Karl, T., Probst, M., Ismailova, O., Winkler, P., Soukoulis, C., Aprea, E., Märk, T., Gasperi, F., and Biasioli, F.: On Quantitative Determination of Volatile Organic Compound Concentrations Using Proton Transfer Reaction Time-of-Flight Mass Spectrometry, Environmental science & technology, 46, 2283-2290, 10.1021/es203985t, 2012.

de Gouw, J., Middlebrook, A., warneke, C., Goldan, P., Kuster, W., Roberts, J., Fehsenfeld, F., Worsnop, D., Pszenny, A., Keene, W., Marchewka, M., Bertman, S., and Bates, T.: Budget of organic carbon in a polluted atmosphere: Results from the New England Air Quality Study in 2002, Journal of Geophysical Research-Atmospheres, 110, D16305, 10.1029/2004JD005623, 2005.

de Gouw, J., and Warneke, C.: Measurements of volatile organic compounds in the earth's atmosphere using proton-transfer-reaction mass spectrometry, Mass Spectrometry Reviews, 26, 223-257, 10.1002/mas.20119, 2007.

de Gouw, J. A., Goldan, P. D., Warneke, C., Kuster, W. C., Roberts, J. M., Marchewka, M., Bertman, S. B., Pszenny, A. A. P., and Keene, W. C.: Validation of proton transfer reaction-mass spectrometry (PTR-MS) measurements of gas-phase organic compounds in the atmosphere during the New England Air Quality Study (NEAQS) in 2002, Journal of Geophysical Research: Atmospheres, 108, 10.1029/2003JD003863, 2003.

de Gouw, J. A., Brock, C. A., Atlas, E. L., Bates, T. S., Fehsenfeld, F. C., Goldan, P. D., Holloway, J. S., Kuster, W. C., Lerner, B. M., Matthew, B. M., Middlebrook, A. M.,

Onasch, T. B., Peltier, R. E., Quinn, P. K., Senff, C. J., Stohl, A., Sullivan, A. P., Trainer, M., Warneke, C., Weber, R. J., and Williams, E. J.: Sources of particulate matter in the northeastern United States in summer: 1. Direct emissions and secondary formation of organic matter in urban plumes, Journal of Geophysical Research: Atmospheres, 113, 10.1029/2007jd009243, 2008.

Gilman, J. B., Lerner, B. M., Kuster, W. C., Goldan, P. D., Warneke, C., Veres, P. R., Roberts, J. M., de Gouw, J. A., Burling, I. R., and Yokelson, R. J.: Biomass burning emissions and potential air quality impacts of volatile organic compounds and other trace gases from fuels common in the US, Atmospheric Chemistry and Physics, 15, 13915-13938, 10.5194/acp-15-13915-2015, 2015.

Guenther, A., Jiang, J., Heald, C., Sakulyanontvittaya, Duhl, T., Emmons, L., and Wang, J.: The Model of Emissions of Gases and Aerosols from Nature version 2.1 (MEGAN2.1): An extended and updated framework for modeling biogenic emissions, Geoscientific Model Development Discussions, 5, 1-58, 10.5194/gmdd-5-1-2012, 2012.

Inomata, S., Tanimoto, H., Kameyama, S., Tsunogai, U., H, I., Kanaya, Y., and Wang, Z.: Technical Note: Determination of formaldehyde mixing ratios in air with PTR-MS: Laboratory experiments and field measurements, Atmospheric Chemistry and Physics Discussions, 8, 10.5194/acpd-7-12845-2007, 2008.

Karl, T., Striednig, M., Graus, M., Hammerle, A., and Wohlfahrt, G.: Urban flux measurements reveal a large pool of oxygenated volatile organic compound emissions, Proceedings of the National Academy of Sciences, 115, 1186-1191, 10.1073/pnas.1714715115, 2018.

Koss, A., Yuan, B., Warneke, C., Gilman, J. B., Lerner, B. M., Veres, P. R., Peischl, J., Eilerman, S., Wild, R., Brown, S. S., Thompson, C. R., Ryerson, T., Hanisco, T., Wolfe, G. M., Clair, J. M. S., Thayer, M., Keutsch, F. N., Murphy, S., and de Gouw, J.: Observations of VOC emissions and photochemical products over US oil- and gas-producing regions using high-resolution H3O+ CIMS (PTR-ToF-MS), Atmospheric Measurement Techniques, 10, 2941-2968, 10.5194/amt-10-2941-2017, 2017.

Koss, A. R., Sekimoto, K., Gilman, J. B., Selimovic, V., Coggon, M. M., Zarzana, K. J., Yuan, B., Lerner, B. M., Brown, S. S., Jimenez, J. L., Krechmer, J., Roberts, J. M., Warneke, C., Yokelson, R. J., and de Gouw, J.: Non-methane organic gas emissions from biomass burning: identification, quantification, and emission factors from PTR-ToF during the FIREX 2016 laboratory experiment, Atmospheric Chemistry and Physics, 18, 3299-3319, 10.5194/acp-18-3299-2018, 2018.

Lopez-Hilfiker, F. D., Mohr, C., Ehn, M., Rubach, F., Kleist, E., Wildt, J., Mentel, T. F., Lutz, A., Hallquist, M., Worsnop, D., and Thornton, J. A.: A novel method for online analysis of gas and particle composition: description and evaluation of a Filter Inlet for Gases and AEROsols (FIGAERO), Atmos. Meas. Tech., 7, 983-1001, 10.5194/amt-7-983-2014, 2014.

Pfannerstill, E. Y., Wang, N., Edtbauer, A., Bourtsoukidis, E., Crowley, J. N., Dienhart, D., Eger, P. G., Ernle, L., Fischer, H., Hottmann, B., Paris, J. D., Stönner, C., Tadic, I., Walter, D., Lelieveld, J., and Williams, J.: Shipborne measurements of total OH reactivity around the Arabian Peninsula and its role in ozone chemistry, Atmos. Chem. Phys., 19, 11501-11523, 10.5194/acp-19-11501-2019, 2019.

Sanchez, D., Seco, R., Gu, D., Guenther, A., Mak, J., Lee, Y., Kim, D., Ahn, J., Blake, D., Herndon, S., Jeong, D., Sullivan, J. T., McGee, T., and Kim, S.: Contributions to OH reactivity from unexplored volatile organic compounds measured by PTR-ToF-MS – A case study in a suburban forest of the Seoul Metropolitan Area during KORUS-AQ 2016, Atmos. Chem. Phys. Discuss., 2020, 1-35, 10.5194/acp-2020-174, 2020.

Sekimoto, K., Li, S.-M., Yuan, B., Koss, A., Coggon, M., Warneke, C., and de Gouw, J.: Calculation of the sensitivity of proton-transfer-reaction mass spectrometry (PTR-MS) for organic trace gases using molecular properties, International Journal of Mass Spectrometry, 421, 71-94, https://doi.org/10.1016/j.ijms.2017.04.006, 2017.

Stark, H., Yatavelli, R. L. N., Thompson, S. L., Kimmel, J. R., Cubison, M. J., Chhabra, P. S., Canagaratna, M. R., Jayne, J. T., Worsnop, D. R., and Jimenez, J. L.: Methods to extract molecular and bulk chemical information from series of complex mass spectra with limited mass resolution, International Journal of Mass Spectrometry, 389, 26-38, https://doi.org/10.1016/j.ijms.2015.08.011, 2015.

Stockwell, C., Veres, P., Williams, J., and Yokelson, R.: Characterization of biomass burning emissions from cooking fires, peat, crop residue, and other fuels with high-resolution proton-transfer-reaction time-of-flight mass spectrometry, Atmospheric Chemistry and Physics, 15, 10.5194/acp-15-845-2015, 2015.

Sulzer, P., Hartungen, E., Hanel, G., Feil, S., Winkler, K., Mutschlechner, P., Haidacher, S., Schottkowsky, R., Gunsch, D., Seehauser, H., Striednig, M., Jürschik, S., Breiev, K., Lanza, M., Herbig, J., Märk, L., Märk, T., and Jordan, A.: A Proton Transfer Reaction-Quadrupole interface Time-Of-Flight Mass Spectrometer (PTR-QiTOF): High speed due to extreme sensitivity, International Journal of Mass Spectrometry, 368, 10.1016/j.ijms.2014.05.004, 2014.

598 Thornton, J., Mohr, C., Schobesberger, S., D'Ambro, E., Lee, B., and Lopez-Hilfiker,
599 F.: Evaluating Organic Aerosol Sources and Evolution with a Combined Molecular
600 Composition and Volatility Framework Using the Filter Inlet for Gases and Aerosols
601 (FIGAERO), Accounts of Chemical Research, 53, 10.1021/acs.accounts.0c00259, 2020.
602 Vlasenko, A., Macdonald, A. M., Sjostedt, S. J., and Abbatt, J. P. D.: Formaldehyde
603 measurements by Proton transfer reaction – Mass Spectrometry (PTR-MS): correction
604 for humidity effects, Atmospheric Measurement Techniques, 3, 1055-1062,
605 10.5194/amt-3-1055-2010, 2010.
606 Wang, C., Wu, C., Wang, S., Qi, J., Wang, B., Wang, Z., Hu, W., Chen, W., Ye, C., Wang,
607 W., Sun, Y., Wang, C., Huang, S., Song, W., Wang, X., Yang, S., Zhang, S., Xu, W., Ma,
608 N., Zhang, Z., Jiang, B., Su, H., Cheng, Y., Wang, X., Shao, M., and Yuan, B.:
609 Measurements of higher alkanes using NO+PTR-ToF-MS: significant contributions of
610 higher alkanes to secondary organic aerosols in China, Atmos. Chem. Phys. Discuss.,
611 2020, 1-32, 10.5194/acp-2020-145, 2020a.
612 Wang, M., Zeng, L., Lu, S., Shao, M., Liu, X., Yu, X., Chen, W., Yuan, B., Zhang, Q.,
613 Hu, M., and Zhang, Z.: Development and validation of a cryogen-free automatic gas
614 chromatograph system (GC-MS/FID) for online measurements of volatile organic
615 compounds, Anal. Methods, 6, 10.1039/C4AY01855A, 2014.
616 Wang, Z., Yuan, B., Ye, C., Roberts, J., Wisthaler, A., Lin, Y., Li, T., Wu, C., Peng, Y.,
617 Wang, C., Wang, S., Yang, S., Wang, B., Qi, J., Wang, C., Song, W., Hu, W., Wang, X.,
618 Xu, W., Ma, N., Kuang, Y., Tao, J., Zhang, Z., Su, H., Cheng, Y., Wang, X., and Shao,
619 M.: High Concentrations of Atmospheric Isocyanic Acid (HNCO) Produced from
620 Secondary Sources in China, Environmental Science & Technology,
621 10.1021/acs.est.0c02843, 2020b.
622 Warneke, C., Veres, P., Holloway, J. S., Stutz, J., Tsai, C., Alvarez, S., Rappenglueck,
623 B., Fehsenfeld, F. C., Graus, M., Gilman, J. B., and de Gouw, J. A.: Airborne
624 formaldehyde measurements using PTR-MS: calibration, humidity dependence, inter-
625 comparison and initial results, Atmospheric Measurement Techniques, 4, 2345-2358,
626 10.5194/amt-4-2345-2011, 2011.
627 Wolfe, G., Marvin, M., Roberts, S., Travis, K., and Liao, J.: The Framework for 0-D
628 Atmospheric Modeling (F0AM) v3.1, Geoscientific Model Development Discussions,
629 1-21, 10.5194/gmd-2016-175, 2016.
630 Yuan, B., Chen, W., Shao, M., Wang, M., Lu, S., Wang, B., Liu, Y., Chang, C. C., and
631 Wang, B.: Measurements of ambient hydrocarbons and carbonyls in the Pearl River

Delta (PRD), China, Atmospheric Research, 116, 93-104, 2012a.
Yuan, B., Shao, M., de Gouw, J., Parrish, D., Lu, S., Wang, M., Zeng, L., Zhang, Q., Song, Y., Zhang, J., and Hu, M.: Volatile organic compounds (VOCs) in urban air: How chemistry affects the interpretation of positive matrix factorization (PMF) analysis, Journal of Geophysical Research (Atmospheres), 117, 24302, 10.1029/2012JD018236, 2012b.
Yuan, B., Koss, A. R., Warneke, C., Coggon, M., Sekimoto, K., and de Gouw, J. A.: Proton-Transfer-Reaction Mass Spectrometry: Applications in Atmospheric Sciences, Chemical Reviews, 117, 13187-13229, 10.1021/acs.chemrev.7b00325, 2017.
Zhang, H., Yee, L. D., Lee, B. H., Curtis, M. P., Worton, D. R., Isaacman-VanWertz, G., Offenberg, J. H., Lewandowski, M., Kleindienst, T. E., Beaver, M. R., Holder, A. L., Lonneman, W. A., Docherty, K. S., Jaoui, M., Pye, H. O. T., Hu, W., Day, D. A., Campuzano-Jost, P., Jimenez, J. L., Guo, H., Weber, R. J., de Gouw, J., Koss, A. R., Edgerton, E. S., Brune, W., Mohr, C., Lopez-Hilfiker, F. D., Lutz, A., Kreisberg, N. M., Spielman, S. R., Hering, S. V., Wilson, K. R., Thornton, J. A., and Goldstein, A. H.: Monoterpenes are the largest source of summertime organic aerosol in the southeastern United States, Proceedings of the National Academy of Sciences, 115, 2038-2043, 10.1073/pnas.1717513115, 2018.
Zhu, M., Dong, H., Yu, F., Liao, S., Xie, Y., Liu, J., Sha, Q., Zhong, Z., Zeng, L., and Zheng, J.: A New Portable Instrument for Online Measurements of Formaldehyde: From Ambient to Mobile Emission Sources, Environmental Science & Technology Letters, 7, 292-297, 10.1021/acs.estlett.0c00169, 2020.